

Analysis of interfacial structure and chemistry in FeV₂O₄-based heterostructures on (001)-oriented SrTiO₃

Y Zhou¹, D Zhou¹, D R G Mitchell², N Valanoor¹ and P Munroe¹

¹ School of Materials Science and Engineering, University of New South Wales, Sydney NSW 2052, Australia

² Electron Microscopy Centre, Australian Institute for Innovative Materials, University of Wollongong, North Wollongong NSW 2522, Australia

E-mail: yanyu.zhou@student.unsw.edu.au

Abstract. In this study, we investigate the interfacial structures and chemistry of FeV₂O₄ (FVO)/SrTiO₃ (STO) and FeV₂O₄/La_{0.33}Sr_{0.67}MnO₃/SrTiO₃ (FVO/LSMO/STO) heterostructures, in which FVO is epitaxially grown on both a (001)-oriented SrTiO₃ substrate and a LSMO-buffered substrate by pulsed laser deposition (PLD). By combining data from transmission electron microscopy (TEM) imaging together with high-resolution scanning transmission electron microscopy (STEM) imaging, the interfaces between FVO and STO, and FVO and LSMO are found to be coherent and semi-coherent, respectively, in spite of more than 8% of strain at the interface. Energy-dispersive X-ray spectroscopy (EDS) analysis suggests that localised diffusion occurs at both the FVO/STO and the FVO/LSMO interfaces.

Introduction

Non-collinear multiferroics (NCMs) are a new class of functional oxides with significant potential in spintronic and nanoelectric application devices, due to their magnetoelectric coupling effects. NCMs produce magnetoelectric coupling by possessing both ferroelectric and ferromagnetic ordering at low temperatures. An NCM, such as FeV₂O₄ (FVO), is a multiferroic which undergoes successive phase transitions and possesses both ferroelectric and ferrimagnetic moments at low temperatures [1, 2].

FVO, in thin film form, has attracted considerable research attention in recent years [3]. Thin-film FVO-based heterostructures exhibit novel properties thought to be associated with the interactions between lattice strain, electronic spin and orbital bonding [2]. Generally, a NCM thin film grown on a ferromagnetic or piezoelectric substrate will lead to large electrical and magnetic properties of the constituent epitaxial thin films [4]. In such thin film heterostructures, the relative lattice parameters of both the substrate and buffer layers play an important role in determining the strain and the structure of the epitaxial thin films. Semi-coherent and incoherent interfaces lead to large dislocation densities, which degrade the ferroelectric properties of these thin films due to the generation of local strain fields [5]. Hence, our aim is to explore the interfacial morphology and chemistry of the FVO-based heterostructures by transmission electron microscopy (TEM) techniques. In this report, epitaxial FVO-based heterostructures were produced by depositing the FVO films onto the STO substrate with, and without, a buffer layer of La_{0.33}Sr_{0.67}MnO₃



(LSMO) using pulsed laser deposition (PLD). These FVO/STO and FVO/LSMO/STO heterostructures were characterised using aberration-corrected scanning transmission electron microscope (STEM). Their interfacial structures were analysed by a combination of bright-field and high-angle annular dark-field (HAADF) imaging. The chemical interactions between the FVO and STO interfaces were investigated using energy-dispersive X-ray spectroscopy (EDS).

Experimental Methods

Two FVO/STO and FVO/LSMO/STO heterostructures were fabricated by PLD. Their crystal structures and surface morphologies were then examined by X-ray diffraction (XRD) and atomic force microscopy (AFM) prior to TEM sample preparation. Cross-sectional TEM specimens that were suitable for both low-magnification TEM and high-resolution STEM imaging were prepared by conventional focused ion beam (FIB) and tripod polishing/ion polishing methods. General microstructural features such as FVO film thickness of the two heterostructures were obtained by analysing FIB specimens using a Philips CM200 field emission TEM. Interfacial structures and chemical interactions of the two heterostructures were investigated by STEM bright-field and HAADF imaging and EDS using a JEOL JEM-ARM200F with tripod-prepared specimens.

Results & Discussion

XRD spectra from FVO/STO and FVO/LSMO/STO confirm the presence of FVO lattice planes in the two grown single-crystalline heterostructures. AFM scans show the mean roughness of the FVO films in the FVO/STO and FVO/LSMO/STO heterostructures was 1.3 nm and 1.5 nm respectively. For brevity neither the XRD nor AFM data are shown here.

A STEM cross-sectional bright-field image of a FVO/STO specimen oriented down at the [100]-zone axis is shown in Figure 1(a). The FVO film is observed to be uniformly distributed along the interface and approximately 75 nm in thickness with a mean surface roughness consistent with the AFM scan. Strain contrast is visible both at the interface and within the FVO film due to the more than 8% of lattice mismatch ($a_{\text{FVO}} = 0.846$ nm [6]; $a_{\text{STO}} = 0.3905$ nm [7, 8]). Higher resolution bright-field and HAADF images at the FVO/STO interface are shown in Figure 1(b) and Figure 1(c) respectively. A reduced fast-Fourier transform (FFT) (Figure 1(b) inset) of a selected area encompassing both the FVO and STO regions, indicates the epitaxial nature and the relaxation of the FVO film in which, the in-plane of the FVO was parallel to that of STO (e.g. $(002)_{\text{STO}} // (004)_{\text{FVO}}$) and the out-of-plane FVO and STO were parallel to each other (e.g. $(020)_{\text{STO}} // (040)_{\text{FVO}}$).

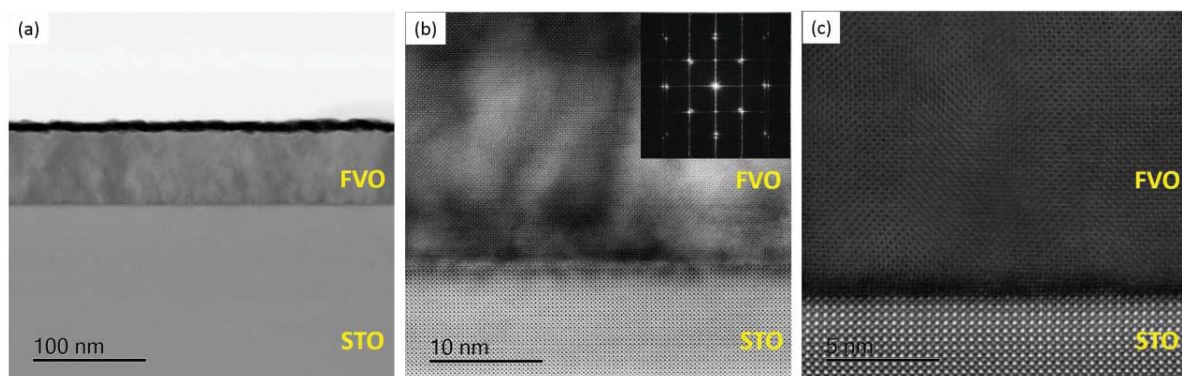


Figure 1. Cross-sectional STEM bright-field images of FVO/STO at (a) low magnification; and (b) high-magnification with reduce FFT inset at zone axis. (c) STEM HAADF image of FVO/STO.

Although no dislocations were observed, they are generally known for relieving the strain induced from the lattice mismatch between the film and the substrate. In order to investigate the possible presence of misfit dislocations, bright-field images of FVO/STO specimen were captured under two beam diffraction conditions, as displayed in Figure 2(a) and 2(b). In Figure 2(a), Moiré fringes were observed along the FVO/STO interface. The average spacing of the Moiré fringes is measured in Figure 2(b) to be 2.98 nm. It suggests the overlapping of the lattice planes

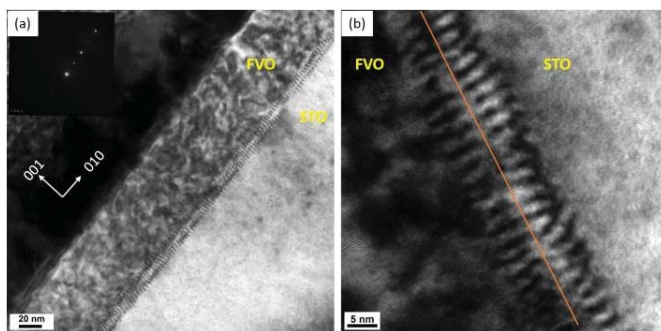


Figure 2. (a) Low-magnification bright-field image of FVO/STO under two beam diffraction conditions ($g = 010$). (b) High-magnification bright-field image of FVO/STO containing Moiré fringes with local spacing measurement inset.

Interfacial diffusion may also play an important role in retaining the epitaxial nature of the FVO film. An EDS line scan across the FVO/STO interface (Figure 3(a) and 3(b)) suggests localised atomic interdiffusion may occur in this region. As the linescan traverses from STO to FVO, the Fe-K and V-K intensities gradually increase over a distance of 3~4 nm, while the Ti-K and Sr-K intensities decrease over the same distance. This EDS line analysis was performed using a JEOL JEM-ARM200F in which the aberration-corrected TEM was operated at a voltage of 200 kV, with a point resolution that could be achieved to less than 0.08 nm. This suggests the gradual change of intensities of Fe-K and V-K is not a result of beam broadening, but rather a case of interdiffusion where Fe and V ions diffuse into the substrate lattice.

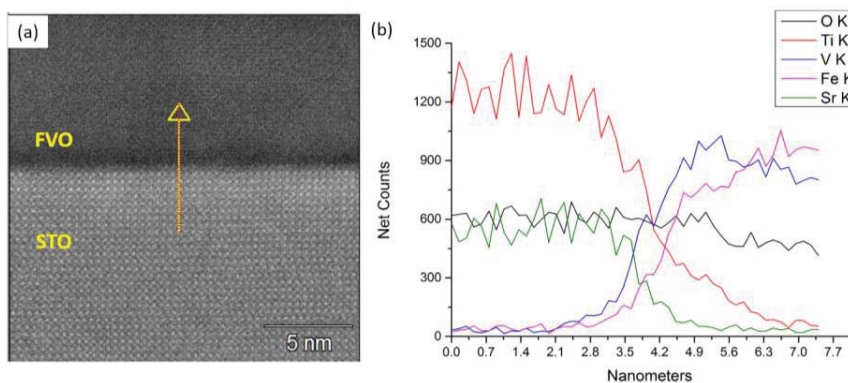


Figure 3. (a) EDS line analysis and scan direction at the interface of FVO/STO specimen. (b) EDS line scan results show gradual increase of the Fe-K and V-K intensities over a distance of 4 nm across the FVO/STO interface.

For the FVO/LSMO/STO sample, a series of STEM bright-field images were captured with the sample oriented parallel to the [100]-zone axis and shown in Figure 4. In Figure 4(a), although the FVO film uniformly grows onto of the LSMO-buffered substrate with a mean surface roughness of 1.5 nm, it appears to obtain low-angle grain boundaries. These low-angle boundaries are more evident at higher magnification (Figure 4(c)) where fringes are observed between neighbouring grains. The inset reduced FFT also shows the tilting of the FVO planes. Due to more than 8% lattice mismatch ($a_{\text{FVO}} = 0.8460$ nm [6]; $a_{\text{LSMO}} = 0.3894$

nm [9]), mismatch dislocations are introduced in the upper region of the LSMO as seen in Figure 4(b). An EDS line scan was also carried out across the FVO/LSMO interface (not shown here) to investigate the changes of intensities of Fe and V across this region. Again, the intensities of Fe-K and V-K signals drop gradually over a distance of 3.5 nm while the Mn-K signal increases, which suggest the occurrence of localised diffusion at this particular interface.

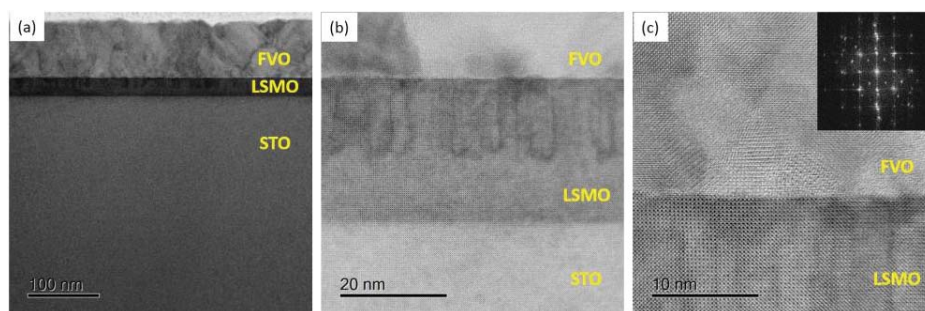


Figure 4. Cross-sectional STEM bright-field images of FVO/LSMO/STO at (a) low magnification and (b) high-magnification showing mismatch dislocations in the LSMO upper layer. (c) STEM bright-field image of FVO/LSMO interface with reduce FFT inset.

Conclusion

Cross-sectional studies of epitaxial FVO/STO and FVO/LSMO/STO by TEM and STEM imaging reveal interdiffusion at interfaces and misfit dislocations play parts to relieve strain due to large lattice mismatches. However, the exact nature of diffusion needs further investigation. Further, EELS studies on the interfaces is required.

Acknowledgement

This research has been supported by the Australia-India Strategic Research Fund (AISRF). The authors would like to acknowledge the facilities, and the scientific and technical assistance, of the Australian Microscopy & Microanalysis Research Facility at the Electron Microscopy Unit, University of New South Wales. This experiment also used equipment funded by the Australian Research Council (ARC) – Linkage, Infrastructure, Equipment and Facilities (LIEF) located at the University of Wollongong Electron Microscopy Centre.

References

- [1] Nii Y, Sagayama H, Arima T, Aoyagi S, Sakai R, Maki S, Nishibori E, Sawa H, Sugimoto K, Ohsumi H and Takata M 2012 *Phys. Rev. B* **86** 125142
- [2] Liu N, Zhao K H, Shi X L and Zhang L W 2012 *J. Appl. Phys.* **111** 124112-5
- [3] MacDougall G J, Garlea V O, Aczel A A, Zhou H D and Nagler S E 2012 *Phys. Rev. B* **86** 060414(R)
- [4] Zheng R K, Wang Y, Liu Y K, Gao G Y, Fei L F, Jiang Y, Chan H L W, Li X M, Luo H S and Li X G 2012 *Mater. Chem. Phys.* **133** 42-46
- [5] Marin L W and Ramesh R 2012 *Acta Mater.* **60** 2449-70
- [6] Zhang Q, Ramazanoglu M, Chi S, Liu Y, Lograsso T A and Vaknin D 2014 *Phys. Rev. B* **89** 224416
- [7] Schlom D G, Chen L -Q, Eom C -B, Rabe K M, Streiffer S K and Triscone J -M 2007 *Annu. Rev. Mater. Res.* **37** 589-626
- [8] Martin L W, Chu Y -H and Ramesh R 2010 *Mater. Sci. Eng. R: Rep.* **68** 89-133
- [9] Lyonnet R, Maurice J L, Hÿtch M J, Michel D and Contour J P 2000 *Appl. Surf. Sci.* **162-163** 245-9